ISSN 0208-7774 TRIBOLOGIA 2/2019 p. 57–64

Wacław GAWĘDZKI[*], Mirosław SOCHA[**]

A METHOD FOR THE DETERMINATION OF THE KINETIC FRICTION COEFFICIENT IN FRICTION PAIRS BASED ON DIRECT ACCELERATION MEASUREMENT OF AN OBJECT ON AN INCLINED PLANE

METODA WYZNACZANIA WSPÓŁCZYNNIKA TARCIA KINETYCZNEGO PAR CIERNYCH W OPARCIU O BEZPOŚREDNI POMIAR PRZYSPIESZENIA OBIEKTU NA RÓWNI POCHYŁEJ

Key words: friction pairs, friction coefficient, acceleration, inclined plane.

Abstract

The paper presents and experimentally verifies a method for the determination of the kinetic friction coefficient of friction pairs. The method involves a direct acceleration measurement of an object sliding down an inclined plane and the determination of the momentary friction force based on acceleration. The laboratory test rig was presented and the theoretical foundations of the method were discussed in detail. The laboratory experiments were conducted for the following material pairs: steel-cast iron, steel-bronze, and for various inclined plane angles. The experiments results were presented, acceleration vs. time curves were plotted, and friction coefficients were determined. These values were compared to the values known from literature **[L. 1–3]**. The uncertainly analysis of kinetic friction coefficient determination was conducted. The method effectiveness and accuracy was verified, noting the sources of possible measurement errors and the ways to eliminate them.

Słowa kluczowe: skojarzenia cierne, współczynnik tarcia, przyspieszenie, równia pochyła.

Streszczenie

W artykule zaproponowano oraz eksperymentalnie zweryfikowano metodę wyznaczania współczynnika tarcia kinetycznego skojarzeń ciernych. Zastosowano metodę bezpośredniego pomiaru przyspieszenia obiektu zsuwającego się po równi pochyłej oraz wyznaczanie na podstawie przyspieszenia chwilowej wartości siły tarcia. Przedstawiono budowę stanowiska laboratoryjnego oraz szczegółowo omówiono podstawy teoretyczne metody. Badania laboratoryjne przeprowadzono dla następujących skojarzeń materiałów: stal–żeliwo, stal–brąz oraz dla różnej wartości kąta równi pochyłej. Zaprezentowano uzyskane wyniki eksperymentów, przebiegi czasowe mierzonych wartości przyspieszeń oraz wartości wyznaczonych współczynników tarcia. Wartości te porównano ze znanymi wartościami z literatury **[L. 1–3]**. Przeprowadzono analizę niepewności wyznaczania współczynnika tarcia kinetycznego. Potwierdzono skuteczność i dokładność metody, zwracając uwagę na źródła możliwych błędów pomiaru oraz możliwość ich eliminacji.

INTRODUCTION

One of important problems of tribological behaviour of friction pairs is their correct mating under the conditions of kinetic friction (brakes, couplings, slide bearings). The mating condition can deteriorate in machinery and equipment drive systems that use the friction between the mating surfaces. When sliding, the coupling discs are subject to heating up and excessive wear and the properties of friction surfaces change. The friction coefficients, both static and kinetic, also change as a result of changes in transmitted torque. The knowledge of frictional characteristics during the operation of mated elements is very important. This is particularly true for static and kinetic friction coefficients that occur on friction pairs. The optimum choice of materials for

[*] ORCID: 0000-0001-5352-0008. AGH University of Science and Technology, Department of Measurement and Electronics, al. A. Mickiewicza 30, 30-059 Krakow, Poland, e-mail: waga@agh.edu.pl.
[**] ORCID: 0000-0001-9462-8269. AGH University of Science and Technology, Department of Measurement and Electronics, al. A. Mickiewicza 30, 30-059 Krakow, Poland, e-mail: socha@agh.edu.pl.

mated friction pairs in couplings, brakes, or slide bearings should take into account the results of laboratory tests evaluating the change of tribological properties during operation.

Literature **[L. 1–3]** presents methods for the determination of static and kinetic friction coefficients, for example, with the use of an inclined plane. For the determination of the kinetic friction coefficient, the inclined plane is at a suitable acute angle α to the horizontal. A specimen of mass m slides down the inclined plane in an accelerated motion, and the acceleration depends on the balance of the following forces acting on the specimen: the sliding force, which is a component of specimen weight, the kinetic friction force, which depends on the specimen weight component, and the kinetic friction coefficient, and an additional force reducing the specimen sliding velocity which is caused by a counterweight, which is a weight on a rope put through a pulley block. The specimen acceleration is determined by measuring the time the specimen takes to travel the set distance while sliding on the inclined plane. Although this method is simple to use, it does not account for factors that are an important source of errors, e.g., the limited accuracy of acceleration determination, the friction force of the rope in the pulley block, or non-axial specimen motion while sliding down the inclined plane.

Contrary to the methods of determination of friction coefficient presented in literature **[L. 4–7]**, this paper suggests and verifies experimentally the method of determination of kinetic friction coefficient using a remote, direct acceleration measurement of the object sliding down an inclined plane and the momentary friction force determined based on the acceleration. The paper presents the laboratory rig to conduct experiments for various friction pairs. The tested pairs included steel, cast iron, and bronze, which are widely used in kinematic nodes of machinery and equipment. The developed method can be used in studies of sliding pairs that require the identification of static and kinetic friction coefficients.

METHOD DESCRIPTION AND TEST RIG DESIGN

Figure 1 shows the test rig used for determination of kinetic friction coefficient in examined pairs.

The rig allows testing selected friction pairs that occur in slide bearings, couplings, and brakes. The design allows the individual subassemblies to be set up quickly and the remote recording of measured acceleration values of an object sliding down the inclined plane.

The rig consists of a base with supports (1) on which the inclined plane (2) is fixed on a rigid structure. The inclined plane is made of C45 steel and is a counter-specimen. The inclined plane length is 1000 mm, width – 40 mm, and thickness – 8 mm. The plane surface is milled 1-mm deep (**Fig. 2**) to form guides for the sliding specimen.

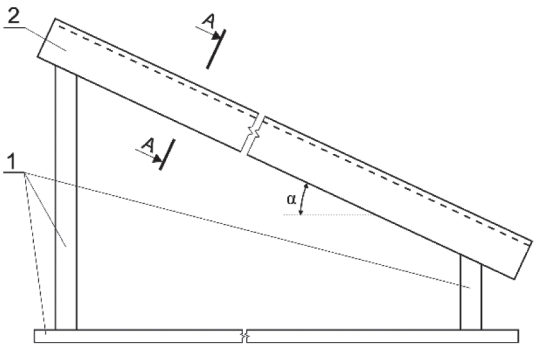

Fig. 1. Test rig for determination of kinetic friction coefficient: 1 – base with supports, 2 – inclined plane, α – inclined plane angle

Rys. 1. Schemat stanowiska do wyznaczania współczynnika tarcia kinetycznego: 1 – podstawa z podporami, 2 – równia pochyła, α – kąt równi pochyłej

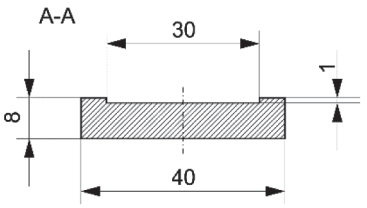

Fig. 2. Inclined plane cross section

Rys. 2. Przekrój poprzeczny równi pochyłej

Figure 3 shows the cross section of the inclined plane (2) illustrating the fixing of specimen (3) in a special enclosure (4) made on a 3D printer that allows an easy installation and removal of the specimen (3) and of the ADXL335 three-axial accelerometer (5).

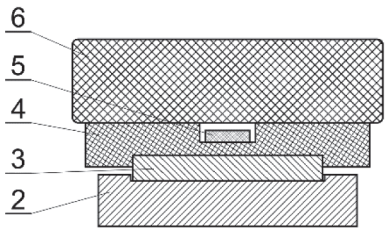

Fig. 3. Cross section of the inclined plane-specimen setup with accelerometer and data transmission system: 2 – inclined plane, 3 – specimen, 4 – specimen and accelerometer enclosure, 5 – accelerometer, 6 – power supply and data transmission system

Rys. 3. Przekrój obiektu równia pochyła–próbka z akcelerometrem i układem transmisji danych: 2 – równia, 3 – próbka, 4 – obudowa próbki i akcelerometru, 5 – akcelerometr, 6 – układ zasilania i transmisji danych

The measurement setup also includes the power supply and wireless data transmission system (6). Two 50 mm × 30 mm × 4 mm specimens were made for the experiments of B6 bronze and EN-GJL-200 cast iron. The specimen dimensions matched the cavity in the enclosure (4). The contact surface with the inclined plane is the specimen material, and the contact surface of the inclined plane is the counter-specimen material.

The use of the inclined plane with variable angle α allows a simultaneous determination of the static friction coefficients of studied pairs. The momentary acceleration values of an object moving in a uniformly accelerated motion on the inclined plane recorded during the experiment allow determining the kinetic friction coefficient of the friction pair.

THEORETICAL FOUNDATIONS OF THE METHOD

The accelerometer converts the measured acceleration to voltage in each of three axes, X, Y, and Z. The sensor scaling has been performed using the gravitational acceleration g by setting in each axis the acceleration $+g$ and $-g$ and reading corresponding voltage values U_{+g} and U_{-g}. The scaling coefficients for the determined sensor supply voltage and for each axis separately are calculated according to the following formulae **[L. 8]**:

$$S = \frac{U_{+g} - U_{-g}}{2g} \tag{1}$$

$$U_{off} = \frac{U_{+g} + U_{-g}}{2} \tag{2}$$

where S – accelerometer conversion sensitivity, U_{off} – offset voltage corresponding to the zero measured acceleration, determined for each axis separately, $g = 9.80665$ ms^{-2} – gravitational acceleration.

Knowing S (1) and U_{off} (2) for individual accelerometer axes, the acceleration values are calculated based on the measured voltage U according to the following formula:

$$a = \frac{U - U_{off}}{S} \tag{3}$$

Figure 4 presents the specimen with the accelerometer in the rest state (specimen blocked) on the sliding plane with angle α to the horizontal and the triaxial acceleration sensor coordinate system XYZ.

Figure 5 illustrates the angles between the sensor axes XYZ and the Earth's gravitational system (one axis is oriented according to the action of gravitational acceleration g, the remaining two axes, perpendicular to the first axis and to each other, form the horizontal plane).

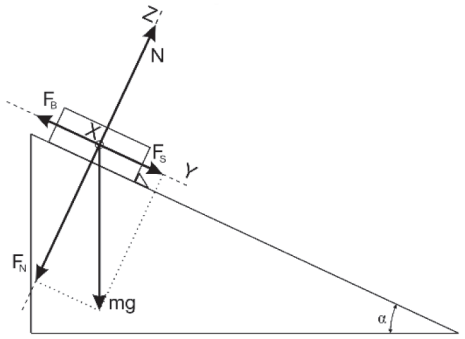

Fig. 4. Specimen with accelerometer in rest state on inclined plate: *mg* – weight, F_N – pressure force, F_S – sliding force, N – substrate reactive force, F_B – blocking reactive force, XYZ – acceleration sensor coordinate system

Rys. 4. Próbka z akcelerometrem w stanie spoczynku na równi pochyłej: *mg* – ciężar, F_N – siła nacisku, F_S – siła zsuwająca, N – siła reakcji podłoża, F_B – siła reakcji blokady ciała na równi, XYZ – układ współrzędnych związany z czujnikiem przyspieszenia

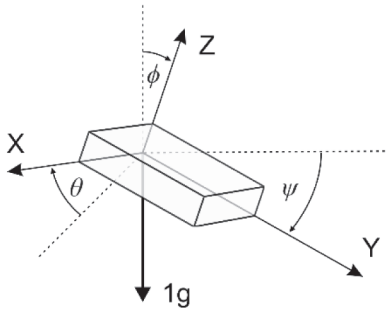

Fig. 5. Angles of the accelerometer coordinate system XYZ relative to the gravitational coordinate system: θ – angle between the accelerometer X axis and horizontal plane, ψ – angle between Y axis and horizontal plane, ϕ – angle between Z axis and the axis of gravitational acceleration *g*

Rys. 5. Kąty nachylenia osi XYZ układu współrzędnych akcelerometru względem grawitacyjnego układu współrzędnych: θ – kąt pomiędzy osią X akcelerometru a poziomem, ψ – kąt pomiędzy osią Y a poziomem, ϕ – kąt pomiędzy osią Z i osią zgodną z kierunkiem działania przyspieszenia ziemskiego g

Angles θ and ψ, between axes X and Y, respectively, and the horizontal plane resulting from gravitational coordinate system (marked with broken lines in **Fig. 5**) and angle ϕ between Z axis and direction of gravitational acceleration g are calculated according to the following formulae **[L. 9]**:

$$\theta = \tan^{-1} \frac{a_x}{\sqrt{a_y^2 - a_z^2}} \tag{4}$$

$$\psi = \tan^{-1} \frac{a_y}{\sqrt{a_x^2 + a_z^2}} \tag{5}$$

$$\phi = \tan^{-1} \frac{\sqrt{a_x^2 + a_y^2}}{a_z} \tag{6}$$

For a theoretical case of perfect inclined plane location relative to the Earth gravitational system, the acceleration values measured in the rest state (**Fig. 4**) are, respectively:

$$a_{x0} = 0\ g,\ a_{y0} = g \sin \alpha_t,\ a_{z0} = g \cos \alpha_t \tag{7}$$

Then, angle α_t for a theoretical case of perfect inclined plane location can be calculated according to the formula (7):

$$\alpha_t = \sin^{-1}\left(\frac{a_{y0}}{g}\right) = \cos^{-1}\left(\frac{a_{yz0}}{g}\right) \tag{8}$$

Angles $\theta_t = 0°$, $\psi_t = \alpha_t$, and $\phi_t = \alpha_t$ can be then calculated according to Formulas (4) to (6) for an actual, non-perfect inclined plane location, angle α_r is calculated according to Formula (5). The inclined plane angle α_r is equal to angle ψ_r between the accelerometer Y axis and gravitational system. The actual inclined plane angle can be calculated using the acceleration measurements in 3 axes a_{x0}, $a_{y0,}$ and a_{z0} in the rest state as follows:

$$\alpha_r = \psi_r = \tan^{-1} \frac{a_{y0}}{\sqrt{a_{x0}^2 + a_{z0}^2}} \tag{9}$$

In the rest state of an object blocked on the inclined plane, the specimen and the accelerometer seismic mass are subjected to action of forces of the same value resulting from the gravitational force component (**Fig. 4**). Force F_s acting on the specimen is compensated by the blocking reactive force F_B, and the identical force F_s acting on the accelerometer seismic mass creates a voltage signal on the accelerometer output that is proportional to acceleration $g \sin \psi_r$. Considering the case of the sliding of the specimen-accelerometer object down the inclined plane (when the blocking is released), let us calculate the balance of forces acting on the object (**Fig. 6**):

$$F = F_s - F_f \tag{10}$$

where F – resultant force acting on the object and causing its uniformly accelerated motion, F_s – sliding force, F_f – friction force.

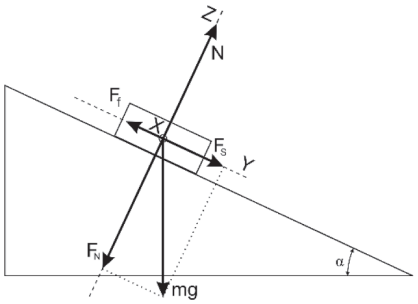

Fig. 6. Distribution of forces acting on the specimen as it slides down the inclined plane: *mg* – weight, F_N – pressure force, F_S – sliding force, N – substrate reactive force, F_f – friction force, XYZ – acceleration sensor coordinate system

Rys. 6. Rozkład sił działających na próbkę podczas zsuwania się po równi pochyłej: mg – ciężar, F_N – siła nacisku, F_S – siła zsuwająca, N – siła reakcji podłoża, F_f – siła tarcia, XYZ – układ współrzędnych związany z czujnikiem przyspieszenia

Expressing the resultant force F (10) acting on the object as appropriate components of gravitational force mg, we obtain the following:

$$ma = mg \sin \psi_r - \mu_k\, mg \cos \psi_r \tag{11}$$

where a – object acceleration during the motion on the inclined plane, m – total object mass, ψ_r – inclined plane angle according to (9), μ_k – kinetic friction coefficient, $g = 9.80665$ ms^{-2} – gravitational acceleration.

The acceleration a_y in axis Y measured by the sensor is

$$a_y = g \sin \psi_r - a \tag{12}$$

and it is equal to the difference of the acceleration $g \sin \psi_r$ acting on the accelerometer seismic mass caused by the constant component of gravitational acceleration along axis Y and the opposite inertia force caused by accelerated motion of the object with acceleration a.

By comparing Equations (11) and (12) we receive the following:

$$a_y = g \sin \psi_r - (g \sin \psi_r - \mu_k\, g \cos \psi_r) = \mu_k\, g \cos \psi_r \tag{13}$$

Hence, the kinetic friction coefficient can be calculated based on Formula (13) according to the following relationship:

$$\mu_k = \frac{a_y}{g \cos \psi_r} \tag{14}$$

where a_y – measured acceleration in axis Y (acc. to (3)), ψ_r – inclined plane angle calculated according to (9).

Using the trigonometric relationship for angles from the first quadrant of the coordinate system

$$\cos\psi_r = \frac{1}{\sqrt{1+\tan^2\psi_r}} \tag{15}$$

and putting it in Formula (14) and using Formula (9) that determines the relationship between the tangent of angle ψ_r and the accelerations, we finally obtain the following:

$$\mu_k = \frac{a_y}{g}\cdot\sqrt{\frac{a_{x0}^2 + a_{y0}^2 + a_{z0}^2}{a_{x0}^2 + a_{z0}^2}} \tag{16}$$

where a_{x0}, $a_{y0,}$ and a_{z0} – accelerations measured in 3 axes in the rest state of the specimen-accelerometer object on the inclined plane, a_y – object acceleration measured while sliding down the inclined plane in a uniformly accelerated motion, and g – gravitational acceleration.

MEASURING SYSTEM

The data acquisition system comprised a NI 9215 four-channel measuring card. It has a 16-bit A/C converter with the voltage measurement range U_{range} = ±10V and the maximum sampling frequency of 100 kHz. The absolute uncertainty of voltage measurement U_{meas} using NI 9215 cards is **[L. 10]**

$$\Delta_U \pm(0{,}02\%\ U_{meas} + 0{,}014\%\ U_{range}) \tag{17}$$

The measuring system featured an NI cDAQ-9191 wireless data transmission (Wi-Fi), and the measurement software was developed in the LabView environment. All system parts are manufactured by National Instruments **[L. 10]**. The accelerometer and the data acquisition and transmission system were supplied from a battery. The acceleration was measured with an ADXL335 integrated accelerometer with ±3 g measuring range and a 0 to 50 Hz frequency range **[L. 11]**. The accelerometer sensitivity S and offset U_{off} for each axis were calculated according to Formulas (1) and (2) during calibration. The calibration accuracy depends on the accuracy of application of standard acceleration ±1 g (ensuring the alignment of sensor axis and gravitational acceleration) and the accuracy of the sensor output voltage measurements U_{+g} and U_{-g} according to (17). Assuming the 1° inaccuracy of determination of the sensor axis and the gravitational acceleration and the accuracy of calibration voltage measurements according to (17), the limit relative uncertainty of sensitivity S according to (1) is δ_S = 0.6 %, and the limit relative uncertainty of offset U_{off} according to (2) is δ_{Uoff} = 0.2 %. The limit absolute uncertainty of acceleration measurements according to (3) is Δ_a = 0.016 g, and the relative limit uncertainty is δ_a = 0.6 % at the 3g measuring range for the accelerometer used. **Table 1** includes the accelerometer calibration coefficients determined according to (1) and (2) for all three axes and for the sensor supply voltage U_{supp} = 3.293 V.

Table 1. Accelerometer calibration coefficients
Tabela 1. Wartości współczynników kalibracyjnych akcelerometru

Parameter	Unit	Axis X	Axis Y	Axis Z
U_{+g}	mV	1952	1959	2058
U_{-g}	mV	1302	1304	1397
S	mV/g	325	327,5	330,5
U_{off}	mV	1627	1631	1727

EXPERIMENTS AND RESULTS

The laboratory experiments were to verify the kinetic friction coefficient determination method of the studied friction pair. Four friction pairs were tested, and the friction was sliding and dry type. The counter-specimen in all experiments was the inclined plane made of C45 steel, and the specimens were made of the following:
- B6 bronze, milled, Ra = 2.5 μm;
- B6 bronze, ground, Ra = 0.63 μm;
- EN-GJL-200 cast iron, milled, Ra = 2.3 μm; and,
- EN-GJL-200 cast iron, ground Ra = 0.57 μm.

The dimensions of paired friction parts are 1000×40×8 mm for the inclined plane sliding surface and 50×30×4 mm for specimens. The total object mass (**Fig. 3**) with the bronze specimen is 921.7 g, and the total mass is 921.1 g with the cast iron specimen (the slight mass difference at various specimen densities is caused by different corner finish).

Each experiment was conducted according to the following pattern:
- The specimen-accelerometer (object) is placed at the highest place of the inclined plane and blocked;
- The measurement procedure is activated in order to record the acceleration signals and control the accelerometer supply voltage;
- After recording the signals in the rest state (accelerations a_{x0}, a_{y0} and a_{z0}), the blocking is removed, and the object slides down the inclined plane and signals are recorded (accelerations a_x, $a_{y,}$ and a_z);
- The experiment ends when the specimen has travelled the entire inclined plane length; and,
- The specimen is changed and the procedure is repeated.

The following recording parameters were used: sampling frequency f_s = 10 kHz, the number of recorded samples N = 32768, and recording time T = 3.2768 s. The experiments were conducted for two different nominal inclined plane angles (α_{1n} = 25° and α_{2n} = 40°), and the actual inclined plane angles were determined during each experiment at the object rest state according to (9).

Figure 7 presents typical acceleration curves in the accelerometer axes X, Y, and Z for the nominal inclined plane angle α_{1n} = 25° recorded for the steel-bronze pair on milled surface, and **Figure 8** – curves for the same pair at the nominal inclined plane angle α_{2n} = 40°. The figures include three acceleration curves for axes Z, Y, and Z. Each figure shows successive experiment phases: object rest state and sliding state. Between them is the transition state during which the object goes from the rest state to the uniformly accelerated sliding motion. The acceleration values a_{x0}, a_{y0}, and a_{z0} (16) are determined based on mean values of each measured acceleration in the rest state. The value a_y (12) in the Y-axis is the mean value of measurement results when the object was sliding down the inclined plane.

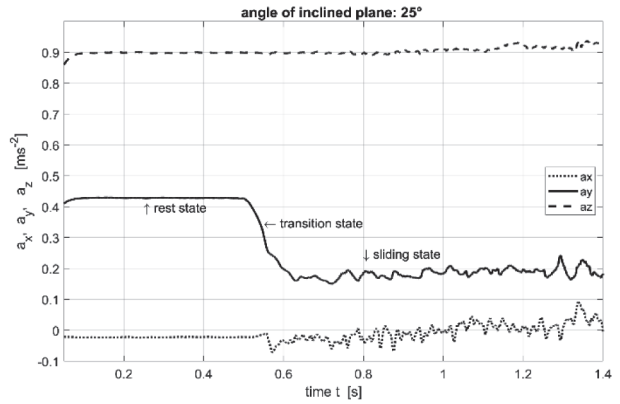

Fig. 7. Acceleration signal curves in axes X, Y, and Z for inclined plane angle α_{1n} = 25°; steel–bronze pair, milled surface

Rys. 7. Przebiegi sygnałów przyspieszeń w osiach X, Y i Z dla kąta równi α_{1n} = 25°, dla skojarzenia: stal–brąz o powierzchni frezowanej

The acceleration values for deferent friction pairs determined during the experiments were used to determine the kinetic friction coefficients according to Formula (16). **Table 2** presents the kinetic friction coefficients and actual inclined plane angles ψ_r (9) determined for two different nominal inclined plane angles α_{1n} = 25° and α_{2n} = 40° and for the following four friction pairs:

– C45 steel – milled bronze,
– C45 steel – ground bronze,
– C45 steel – milled cast iron, and
– C45 steel – ground cast iron.

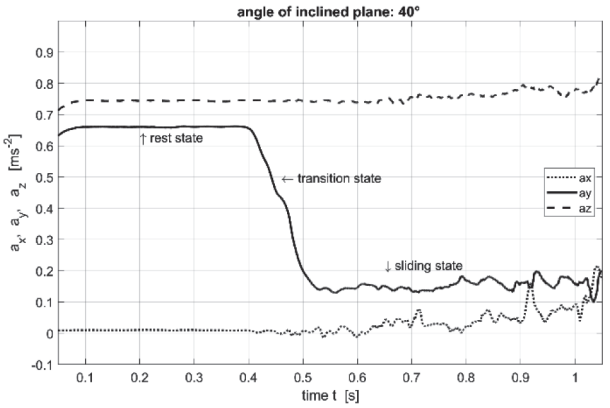

Fig. 8. Acceleration signal curves in axes X, Y, and Z for inclined plane angle α_{1n} = 40°; steel–bronze pair, milled surface

Rys. 8. Przebiegi sygnałów przyspieszeń w osiach X, Y i Z dla kąta równi α_{1n} = 40°, dla skojarzenia: stal–brąz o powierzchni frezowanej

The limit, absolute uncertainty of kinetic friction coefficient determination based on (16) was calculated using the total differential method, assuming the absolute uncertainty of acceleration measurement Δ_a = 0.016 g determined in the section on the measuring system. The uncertainty limit value was determined for experiments are shown in **Figures 7** and **8**, and the results are presented in **Table 2** for the following:

– The inclined plane angle α_{1n} = 25°,
– The kinetic friction coefficient determination uncertainty $\Delta\mu_k$ = 0.018,
– The inclined plane angle α_{1n} = 40°,
– The kinetic friction coefficient determination uncertainty $\Delta\mu_k$ = 0.020.

Table 2. Determined kinetic friction coefficients

Tabela 2. Wyznaczone wartości współczynników tarcia kinetycznego

Friction pair	α_{1n} = 25°		α_{2n} = 40°	
	ψ_r	μ_k	ψ_r	μ_k
C45 steel – milled bronze	25.4°	0.21 ±0.018	41.8°	0.23 ±0.02
C45 steel – ground bronze	25.7°	0.20 ±0.018	41.5°	0.22 ±0.02
C45 steel – milled cast iron	25.0°	0.19 ±0.018	40.9°	0.14 ±0.02
C45 steel – ground cast iron	25.0°	0.14 ±0.018	41.1°	0.11 ±0.02

ANALYSIS OF RESULTS

The approximate kinetic friction coefficients μ_k for the steel-cast iron pair given in literature are about 0.18 **[L. 1, 3, 12]**, and for the steel-bronze pair, they are also about 0.18 **[L. 1, 3, 13]**. The impact of surface quality on coefficients was tested for each pair. **Table 2** indicates that, for the milled steel-bronze pair, the values of kinetic friction coefficient are similar, from 0.2 to 0.23, regardless of the bronze surface roughness, milled or ground. The values are close to the upper limit typical for such materials; however, the surfaces of the tested friction pairs were machined: milled or ground. The kinetic friction coefficient for milled bronze is greater than for the ground bronze, similarly as for the milled steel-cast iron pair. However, in the case of that second pair, the difference between milled and ground cast iron is quite significant and reaches maximum values typical for this type of friction pairs. The inclined plane angle is also important in this method: At a lesser angle, the object slides down slower, and, at a greater angle, it slides down faster. For the lesser inclined plane angle, the measurement sensitivity will be lower because of the smaller difference between the accelerations measured at the rest state and at the sliding state (e.g., in **Fig. 7** for $\alpha_{1n} = 25°$ and in **Fig. 8** for $\alpha_{2n} = 40°$). The greater the angle, the greater is the acceleration during the sliding state, which increases the velocity and instability of the sliding object as shown in **Figs. 7** and **8**. The analysis of data from **Table 2** indicates that dispersion of the determined values of kinetic friction coefficient μ_k during individual experiments is within the calculated measurement uncertainty $\Delta\mu_k$.

CONCLUSIONS

The paper presents a laboratory rig design, theoretical foundations for the method of kinetic friction coefficient determination, and examples of results of laboratory experiments for various friction pairs. The following conclusions can be formulated based on the studies:

- Studies of four different friction pairs made of steel, cast iron, and bronze proved the effectiveness of the proposed method for determination of kinetic friction coefficient with high accuracy.
- The inclined plane angle is important in this method, due to conflicting requirements in relation to the high sensitivity of acceleration measurement and resistance to interference caused by instability of the object sliding down the inclined plane.
- Recording and visualization of momentary acceleration values in three axes (**Figs. 7** and **8**) is a basis for analysis of occurring phenomena in order to choose the correct inclined plane angle.
- The static friction coefficient can also be determined after a slight modification of the inclined plane design.
- The use of a different integrated sensor that, in addition to the accelerometer also includes a gyroscope, magnetometer, all in a three-axial system, will allow measuring the momentary value of the angle between the axes of the accelerometer coordinate system and the gravitational system. This will allow eliminating the errors caused by instability of the motion of the object sliding down the inclined plane and increasing the accuracy of determination of kinetic friction coefficient.

This research was financed by resources for research activities of the Department of Metrology and Electronics, AGH, no. 16.16.120.773.

REFERENCES

1. Standard Guide for Measuring and Reporting Friction Coefficients, ASTM Annual Book of Standards, Volume 03.02, ASTM International, West Conshohocken, PA, 2008, pp. 492–503.
2. Blau P.J.: The significance and use of the friction coefficient. Tribol Int 34(9), 2001, pp. 585–591.
3. Blau P.J.: Friction Coefficient. In: Wang Q.J., Chung YW. (eds) Encyclopedia of Tribology. Springer, 2013 Boston, MA.
4. Lepiarczyk D., Tarnowski J., Gawędzki W.: The stand for measurement of kinetic and static friction coefficient in friction pairs, Bimonthly Tribologia 2009, 228 (6), pp. 69–79.
5. Tarnowski J., Gawędzki W., Lepiarczyk D.: Determination of the slide bearing friction coefficient on the basis of heat balance, Bimonthly, Tribologia 2011, 240 (6), pp. 219–225.
6. Konopka S., Kolankowska E.: Methodological aspects of determining the coefficient of kinetic friction of wheat kernels on an inclined plane, Bimonthly Tribologia, 2018, 278 (2), pp. 45–50.

7. Ming-Hsiang Shih, Wen-Pei Sung: Developing Smart Measurement Device to Measure Kinetic Friction Coefficients of Bi-Tilt Isolator, Advances in Civil Engineering, Vol. 2019, Article ID 4392506, 12 pages.
8. Gawędzki W.: Pomiary elektryczne wielkości nieelektrycznych. Wydawnictwa AGH, Kraków 2010.
9. Application Note AN-1057: Using an accelerometer for inclination sensing, Analog Devices, http://www.analog.com.
10. Datasheet NI9215, NI cDAQ-9191, National Instruments, http://www.ni.com.
11. Datasheet ADXL335, Analog Devices, http://www.analog.com.
12. Fischer U., et al., Poradnik mechanika. Wyd. REA, Warszawa 2008.
13. Stöcker H., Nowoczesne kompendium fizyki. PWN Warszawa 2010.